# Topography of the Hydrophilic Helices of Membrane-Inserted Diphtheria Toxin T Domain: TH1−TH3 as a Hydrophilic Tether†

Jie Wang, Michael P. Rosconi, and Erwin London*

*Department of Biochemistry and Cell Biology and Department of Chemistry, State University of New York (SUNY)−Stony Brook, Stony Brook, New York 11794-5215*

*Received March 24, 2006; Revised Manuscript Received May 3, 2006*

ABSTRACT: After low pH-triggered membrane insertion, the T domain of diphtheria toxin helps translocate the catalytic domain of the toxin across membranes. In this study, the hydrophilic N-terminal helices of the T domain (TH1−TH3) were studied. The conformation triggered by exposure to low pH and changes in topography upon membrane insertion were studied. These experiments involved bimane or BODIPY labeling of single Cys introduced at various positions, followed by the measurement of bimane emission wavelength, bimane exposure to fluorescence quenchers, and antibody binding to BODIPY groups. Upon exposure of the T domain in solution to low pH, it was found that the hydrophobic face of TH1, which is buried in the native state at neutral pH, became exposed to solution. When the T domain was added externally to lipid vesicles at low pH, the hydrophobic face of TH1 became buried within the lipid bilayer. Helices TH2 and TH3 also inserted into the bilayer after exposure to low pH. However, in contrast to helices TH5−TH9, overall TH1−TH3 insertion was shallow and there was no significant change in TH1−TH3 insertion depth when the T domain switched from the shallowly inserting (P) to deeply inserting (TM) conformation. Binding of streptavidin to biotinylated Cys residues was used to investigate whether solution-exposed residues of membrane-inserted T domain were exposed on the external or internal surface of the bilayer. These experiments showed that when the T domain is externally added to vesicles, the entire TH1−TH3 segment remains on the cis (outer) side of the bilayer. The results of this study suggest that membrane-inserted TH1−TH3 form autonomous segments that neither deeply penetrate the bilayer nor interact tightly with the translocation-promoting structure formed by the hydrophobic TH5−TH9 subdomain. Instead, TH1−TH3 may aid translocation by acting as an A-chain-attached flexible tether.

Diphtheria toxin (DT), a cytotoxic protein with 535 amino acid residues, is secreted by pathogenic strains of *Corynebacterium diphtheriae*. The three-dimensional structure of DT in solution at neutral pH was first solved by Choe et al. (*4*). This study showed that the toxin consists of a catalytic domain (C), a membrane-inserting translocation domain (T), and a receptor-binding domain (R). The protein is secreted as a single polypeptide chain and is then cleaved at residue 193 between the C and T domains by a protease, likely furin, to create an active form (*5*, *6*). This cleavage event yields a N-terminal A chain (equivalent to the catalytic domain) linked by a disulfide bond to a C-terminal B chain composed of the T and R domains.

The killing action of DT involves several distinct steps. The first steps involve binding to a receptor [a membrane-anchored version of a heparin-binding epidermal-growth-factor-like protein (*7*)] on the surface of sensitive cells and subsequent receptor-mediated endocytosis. Translocation of the A chain of the toxin across the endosomal membrane and into the cytoplasm of the cell is induced by the acidic environment inside the endosome (*8*). After translocation, the A chain catalyzes the transfer of an ADP-ribosyl group from $NAD^+$ to a specific modified histidine (diphthamide) of protein synthesis elongation factor 2, thus inhibiting protein synthesis and leading to cell death (*9*).

Exposure to endosomal low pH aids translocation by triggering a conformational change that exposes hydrophobic sequences in the T domain and membrane insertion (*10*). The T domain is thought to be primarily responsible for insertion, although the A chain and R domain also have some ability to associate with membranes (*11*−*17*). It has been shown that the T domain is capable of translocating the A chain across planar phospholipid bilayers in the absence of other proteins, and thus, it appears to contain the molecular machinery for mediating translocation (*18*). The T domain is a pore-forming protein (*19*−*22*) that interacts with proteins in the molten-globule state, including the A chain, and may act as a transmembrane chaperone (*23*, *24*). However, exactly how T domain assists translocation is unclear. Furthermore, translocation may be aided by cytoplasmic factors (*25*, *26*).

Defining the structure of the membrane-inserted T domain is likely to provide insights into the mechanism of A chain translocation. The T domain is primarily comprised of 9 α helices (TH1−TH9). In the native state in solution, hydrophobic helices TH8 and TH9 form a largely buried core, semi-hydrophobic helices TH5−TH7 are on the T domain surface that is normally somewhat protected from exposure to solution by the R domain, and the relatively hydrophilic

† This work was supported by NIH Grant GM 31986.

* To whom correspondence should be addressed. Telephone: 631-632-8564. Fax: 621-632-8575. E-mail: erwin.london@stonybrook.edu.

10.1021/bi060587f CCC: $33.50 
Published on Web 06/10/2006

helices TH1−TH4 are the most exposed to aqueous solution (*4*).

The conformation of the membrane-inserted T domain has been only partially defined. The membrane-inserted T domain can exist in shallowly (P state) and deeply (TM state) inserted conformations (*2*, *3*, *27*, *28*). The formation of the TM state is promoted by a high concentration of T domain in the membrane, a thin bilayer width, and interactions with molten-globule conformation proteins (*2*, *3*, *23*, *27*, *28*). In the TM state, the TH8−TH9 region is proposed to insert in the form of a transmembrane hairpin (*4*, *27*, *29*, *30*), while in the P state, it lies close to the surface of the bilayer. TH8 and TH9 are connected by a short loop (TL5) containing acidic residues whose protonation has been proposed to aid membrane insertion (*4*, *27*, *31*). TH8 and TH9 also are critical for and at least under some conditions sufficient for pore formation (*22*, *29*, *32*, *33*). Similar to TH8−TH9, TH5−TH7 insert shallowly in the P state and deeply in the TM state (*1*). However, even though TH5 and TH6−TH7 are long enough to form TM segments, they do not form a TM hairpin in either the P or TM states and the loop connecting TH5−TH6 remains exposed on the cis side of the bilayer (the side from which insertion occurs). Interestingly, disruption of deep insertion of TH8−TH9 disrupts deep insertion of TH5−TH7, indicating that the TH8−TH9 and TH5−TH7 regions interact with each other in the deeply inserted conformation (*34*). Thus, it is possible that TH5−TH7 form part of the walls of the translocation path through the membrane. However, the exact role of TH5−TH7 in translocation is unknown.

Although TH1−TH4 are not necessary for T domain pore formation (*22*, *35*), previous studies do indicate that these more hydrophilic N-terminal helices have some role in translocation. The N-terminal region of the T domain is connected to the A chain though a disulfide bond, and previous studies indicate that the translocation of the N terminal end of the T domain and the C terminal end of the A domain is the initial step in translocation (*36*). In addition, the N-terminal helices are required for efficient delivery of the A chain to the cell cytosol (*37*). Mutagenesis studies show that the amphiphilic pattern of residues within TH1, rather than the precise identity of the amino acids, is essential for T domain function (*38*). In addition, this study showed that insertion of a charged residue in the hydrophobic face of TH1 knocked out DT toxicity, while such a mutation in the hydrophilic face did not. Translocation of the A chain was strongly inhibited when charged residues on TH1 were replaced with uncharged ones, but this did not affect channel activity (*39*). This indicates that hydrophobic contacts made by TH1 are not sufficient for function. On the basis of these observations, it was suggested that TH1 might act as a recognition sequence for the translocation machinery and that this interaction was probably the first step in the translocation process.

In this study, the low pH conformation of the N-terminal segment of the T domain in solution and its topography when inserted into model membrane vesicles was investigated to complete topographical analysis of the T domain. The results show that there is a major change in TH1 conformation in solution upon exposure of the T domain to low pH. Upon addition to lipid bilayers, all of the helices in the N-terminal part of the T domain shallowly insert into membranes. Importantly, the topography of the membrane-inserted N-terminal segment is not linked to that of the C-terminal region. The implications of this observation for the A chain translocation mechanism are discussed.

## EXPERIMENTAL PROCEDURES

*Materials.* 1,2-Dioleoyl-*sn*-glycero-3-phospholcholine (DOPC), 1,2-dimyristoleoyl-*sn*-glycero-3- phosphocholine (DMoPC), and 1,2-dioleoyl-*sn*-glycero-3-phosphoglycerol (DOPG) were purchased from Avanti Polar Lipids (Alabaster, AL). 10-Doxylnonadecane (10-DN) was obtained by custom synthesis (Molecular Probes, Eugene, OR). Lipid concentrations were determined by dry weight. Rabbit anti-BODIPY-FL IgG, *N*-[(4,4-difluoro-5,7-dimethyl-4-bora-3a,-4a-diaza-*s*-indecene-3-yl)methyl]iodoacetamide (BODIPY-FL C1-IA, BODIPY-IA), monochlorobimane, and rhodamine B-1,2-dihexadecanoyl-*sn*-glycero-3-phosphoethanolamine triethylammonium salt (Rho-DHPE) were purchased from Molecular Probes (Eugene, OR). *Pfx* polymerase, the restriction enzymes *Eco*R I and *Nde* I, synthetic oligonucleotides, alkaline phosphatase, and T4 ligase were purchased from Invitrogen (Rockville, MD). Human serum albumin (HSA) was obtained from Worthington Biochemical (Lakewood, NJ). All other chemicals were reagent-grade.

*Site-Directed Mutagenesis. Escherichia. coli* BL-21 cells containing wild-type (WT) T domain inserted into the pET 15b plasmid were obtained from the lab of Dr. John Collier (Harvard Medical School). The pET 15b vector contains a gene for ampicillin resistance and encodes for a 20 residue N-terminal tag containing a hexahistidine sequence (*1*, 22). Two-step (asymmetric) polymerase chain reaction (PCR) was used as previously described (*1*), except using complementary primers 30−33 base pairs in length and containing the desired single amino acid mutation. Mutations were confirmed by automated DNA sequencing (Center for the Analysis and Sequence of Macromolecules, SUNY, Stony Brook, NY). To improve expression levels for the T domain containing Cys mutations at residues 218, 241, or 254, the T-domain-coding insert was removed by digestion with restriction enzymes *Eco*R I and *Nde* I and inserted into a pET28a vector, which contains a kanamycin resistance gene.

*Expression and Purification of T Domain Mutants.* Mutant T domain proteins were overexpressed and isolated from *E. coli* basically as previously described (*1*, *2*). Ampicillin concentrations of 100−200 $\mu$g/mL were used to increase plasmid stability. Kanamycin (50 $\mu$g/mL) was used to select plasmid-containing bacteria for mutants 218, 241, and 254 (*17*, *34*). Mutant proteins were purified from an *E. coli* extract as previously described (*1*, *3*, *22*). The first step involved affinity chromatography using a Talon metal-affinity resin (CLONTECH, Palo Alto, CA). In the second step, proteins were treated with dithiothreitol and then subjected to fast protein liquid chromatography (FPLC) with a Source Q anion-exchange column (*1*, *17*, *22*). The collected fractions were run on sodium dodecyl sulfate−polyacrylamide gel electrophoresis (SDS−PAGE) gel to monitor the elution position and purity of the protein. Final purity appeared to be above 95% in all cases. Protein concentrations were determined by the Bio-Rad protein assay (Bradford method) (*40*). For the T domains, this gives values roughly 10−12% higher compared to that estimated by native protein absor-

bance at 280 nm (*3*). Final protein concentrations were corrected to values that would have been obtained by absorbance at 280 nm.

*Fluorescence Labeling of T Domain Mutants.* Monochlorobimane and BODIPY-IA were used to label single Cys T domain mutants as described previously (*1*, *3*). For mutants with Cys residues buried within the interior of the T domain in solution at neutral pH (T213C and A254C), 4 M urea was added to the purified protein to unfold it and expose the Cys residue for labeling (*3*). After 30 min of incubation with the label at room temperature, samples were diluted 20-fold with 20 mM Tris-HCl buffer at pH 8.0. They were then separated from the free label, and at the same time the protein was concentrated by FPLC with a Source Q anion-exchange column. The column was washed with 10 mM Tris at pH 8.0 and then eluted with an increasing salt gradient (10 mM Tris at pH 8.0 and 0−0.5 M NaCl). Fractions were run on a SDS−PAGE gel to identify fractions containing protein. Samples of WT T domain were labeled in parallel with the Cys mutants to assay nonspecific labeling, and fluorescence measurements were used to compare the relative labeling efficiency of the mutant and WT protein. To avoid interference from nonspecific labeling of residues other than Cys, only preparations in which labeling efficiency was at least 20 times greater than WT T domain were used (with the exception of the T domain with a Cys at position 210, for which labeling efficiency was 15-fold over WT).

*Preparation of Model Membrane-Incorporated T Domain.* T domain was incorporated into sonicated small unilamellar vesicles (SUVs), composed of DOPC/DOPG (70 mol % DOPC and 30 mol % DOPG) or DMoPC/DOPG (70 mol % DMoPC and 30 mol % DOPG) as described previously (*3*). Unless otherwise noted, the final concentration of lipid was 200 $\mu$M and the lipids were dispersed in 167 mM acetate, 6.7 mM Tris-HCl, 150 mM NaCl at pH 4.3 (buffer A). In most experiments, the final concentration of protein was 2 $\mu$g/mL for bimane-labeled protein and 1 $\mu$g/mL for BODIPY-labeled protein. The sample volume was 800 $\mu$L. For mutants that labeled relatively poorly with bimane (L220C and E241C), both SUV and protein concentrations used were doubled. Samples in which additional unlabeled WT T domain (WT T, 8 $\mu$g/mL) or HSA (5 $\mu$g/mL) were added were also prepared as described previously (*1*, *3*)

*Fluorescence Measurements.* Fluorescence was measured on a Spex Tau-2 Fluorolog spectrofluorimeter operating in steady-state ratio mode using a semi-micro quartz cuvette (excitation path length of 10 mm and emission path length of 4 mm). The excitation and emission slits were set to 2.5 and 5.0 mm, respectively. Bimane fluorescence was measured with an excitation wavelength of 375 nm. Bimane emission spectra were measured from 420 to 520 nm at a rate of 1 nm/s. BODIPY fluorescence was measured for 10 s with an excitation wavelength of 485 nm and emission wavelength of 515 nm. In all cases, background intensities from samples lacking protein were subtracted from the intensities measured in protein-containing samples. All measurements were made at room temperature unless otherwise noted.

Anti-BODIPY antibody binding experiments were performed as described previously (*1*, *3*). For each sample, four measurements were made both before and after antibody addition, mixing samples between measurements. For anti-body addition, a 20 $\mu$L aliquot of anti-BODIPY antibodies (from a 3 mg/mL commercial stock solution dissolved in phosphate-buffered saline at pH 7.2 and 5 mM azide) was added to each sample and mixed. Fluorescence intensity was then measured after 30 min of incubation at room temperature.

*Dual Quenching Experiments To Measure the Relative Depth of Bimane-Labeled Residues.* For measurement of the depth of bimane-labeled residues within the bilayer, iodide and 10-DN quenching of bimane was measured as described previously (*17*). Samples were prepared by incorporating bimane-labeled T domain into 7:3 (mol/mol) DOPC/DOPG or DMoPC/DOPG SUVs in buffer A at pH 4.3 as described above. The fluorescence emission intensity at 467 nm was measured before and after the addition of 50 $\mu$L of freshly prepared 1.7 M KI containing 0.85 mM sodium dithionite. A second set of samples was prepared with the same lipid concentrations (200 $\mu$M) plus 10 mol % (for DOPC-containing vesicles) or 7.8 mol % (for DMoPC-containing vesicles) 10-DN. Bimane fluorescence in the presence of 10-DN was then compared to that in its absence. Quenching by iodide ($F_o/F_{KI} - 1$), 10-DN ($F_o/F_{10-DN} - 1$), and 10-DN/iodide quenching ratio $(F_o/F_{10-DN} - 1)/(F_o/F_{KI} - 1)$ was then calculated (after the correction for dilution by the iodide-containing aliquot, where appropriate). In these formulas, $F_o$ is the fluorescence in the absence of the quencher, $F_{KI}$ is the fluorescence in the presence of KI, and $F_{10-DN}$ is the fluorescence in the presence of 10-DN. In all cases, these fluorescence intensities were corrected for fluorescence intensities in background samples lacking protein.

*Interaction of Biotinylated T Domain Mutants with Externally Added and Vesicle-Trapped BODIPY−Streptavidin.* Vesicles containing trapped BODIPY−streptavidin (BOD−SA), trapped streptavidin (SA), or no trapped protein were prepared as described previously (*22*). A mixture was prepared containing 10 mM lipid composed of 70 mol % DOPC, 30 mol % DOPG, 0.002 mol % Rho-DHPE, plus 100 $\mu$g/mL BOD−SA or SA, and 20 mg/mL *n*-octyl-$\beta$-glucoside, all dissolved in 10 mM Tris-HCl and 150 mM NaCl at pH 8.0 (*22*). After *n*-octyl-$\beta$-glucoside was removed by dialysis, mixtures containing trapped protein were applied to a Sepharose CL-4B column (1 cm in diameter and 50 cm in length) to separate free from large unilamellar vesicle (LUV)-entrapped BOD−SA or SA. After elution with buffer A, fractions containing LUVs were collected. Fractions containing free BOD−SA were also collected for later use as externally added BOD−SA (see below). Vesicles and protein were detected as described previously (*22*). The final concentrations of BOD−SA and lipid were determined by measurement of the BODIPY and Rho-DHPE fluorescence, respectively. Typical final concentrations were 2.5−5 mM lipid and 5.6−8.0 $\mu$g/mL entrapped BOD−SA or 2.3−5.7 mM lipid and 3.8−6.5 $\mu$g/mL entrapped SA. The chromatography step was omitted for vesicles without trapped protein.

The T domain was biotin-labeled, and biotinylated protein was separated from unbiotinylated protein as described previously (*22*). The reactivity of the membrane-inserted T domain with BOD−SA was then measured similarly as previously described (*22*), except pH was 4.3. Reactivity was measured under three different conditions: (1) with externally added BOD−SA (BOD−$SA_{ex}$ samples), (2) with

trapped BOD−SA (BOD−$SA_{tr}$ samples), and (3) with externally added BOD−SA and trapped unlabeled SA (BOD−$SA_{ex}$/$SA_{tr}$ samples).

For BOD−$SA_{tr}$ samples, LUVs containing trapped protein were diluted to just under 700 $\mu$L with buffer A to give a concentration of 0.2 $\mu$g/mL entrapped BOD−SA. BODIPY fluorescence was measured, and then a small aliquot (1−5 $\mu$L) of concentrated T domain was added to give a final concentration of 0.2 $\mu$g/mL biotinylated plus 1.8 $\mu$g/mL unbiotinylated WT T domain and a total volume of 700 $\mu$L. The final lipid concentration, which varied because trapping efficiency was variable, was in the range of 1.4−1.8 mM. After incubation for 30 min, BODIPY fluorescence was remeasured.

For the BOD−$SA_{ex}$ and BOD−$SA_{ex}$/$SA_{tr}$ samples, BODIPY fluorescence was first measured in a 630 $\mu$L sample containing BOD−SA diluted to 0.2 $\mu$g/mL with buffer A. Then, 70 $\mu$L of the appropriate T domain−LUV mixture was added, and fluorescence was measured after an incubation of 30 min. The T domain−LUV mixture contained the T domain preincubated for 15 min with LUVs (with or without trapped unlabeled streptavidin) and buffer A to give the same final T domain and lipid concentrations as the samples with trapped BOD−SA.

To evaluate the percent exposure of the biotinylated residues on the outside surface of the vesicles, the percent external reactivity was calculated. Percent external activity $= \{(F - F_o)_{ex}/[(F - F_o)_{ex} + (F - F_o)_{tr}]\} \times 100\%$, where $F_o$ is the BOD−SA fluorescence intensity prior to the addition of the T domain to BOD−SA containing solution, and $F$ is the BOD−SA fluorescence intensity 30 min after incubation of the T domain with BOD−SA. $(F - F_o)_{ex}$ is the increase in BODIPY fluorescence intensity in the presence of the biotinylated T domain in samples containing externally added BOD−SA, and $(F - F_o)_{tr}$ is the increase in BODIPY fluorescence in the presence of the T domain in samples containing trapped BOD−SA. Background intensities from samples lacking BOD−SA were subtracted to obtain BODIPY fluorescence intensities. For external BOD−SA experiments, BODIPY fluorescence values were corrected for dilution by the vesicle-containing aliquot.

## RESULTS

*Bimane and BODIPY Topography Assays.* The aim of this study was to complete the analysis of the topography of the membrane-inserted T domain. To do this, single Cys residues were introduced at various positions in helices TH1−TH3. Because previous studies have proposed that the interaction of helix TH1 with membranes is important for translocation, its topography was studied in detail, with residues located on both the more hydrophobic face (213, 216, and 220) and more hydrophilic face (208, 210, 211, 215, 218, and 221) of TH1. The other residues studied were 203, which is near the N terminus of the T domain, residue 228 in helix TH2, and residues 241 and 254 in helix TH3. The single Cys mutants were labeled with fluorescent bimane or BODIPY groups (*1*, *3*). It was previous shown that bimane and BODIPY-labeled T domain behaves similarly to the WT protein (*1*−*3*, *17*, *22*). Consistent with the behavior of the WT protein, the labeled T domain underwent a conformation change at low pH and retained the ability to interact with lipid bilayers at low pH (see below).

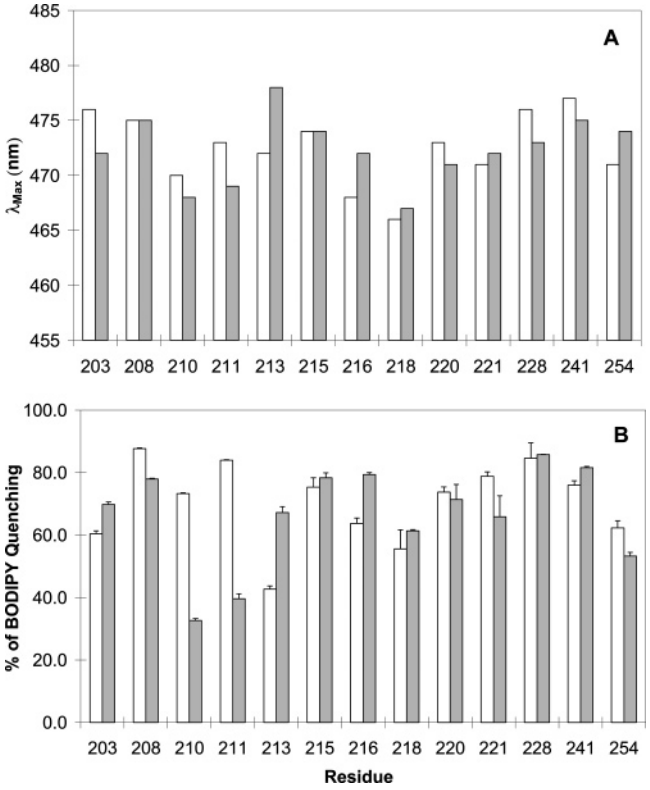


FIGURE 1: Fluorescence properties of labeled T domain in solution. (A) Wavelength of the maximum emission ($\lambda_{max}$) of bimane fluorescence for labeled T domain at pH 8.0 (open bars) and 4.3 (shaded bars). (B) Percent quenching of BODIPY fluorescence by anti-BODIPY antibody with labeled T domain at pH 8.0 (open bars) and 4.3 (shaded bars). Percent quenching was calculated using the formula $(1 - (F/F_o)) \times 100\%$, where $F_o$ is the fluorescence intensity before the addition of the antibody and $F$ is the fluorescence intensity 30 min after the antibody addition. Numbers on the *x* axis indicate positions of labeled Cys residues. Unless otherwise noted, in all figures the average value from duplicate samples is shown. The error bars represent the standard deviation of the mean, which is the standard deviation divided by the square root of the number of samples. $\lambda_{max}$ values in this and all following figures were generally reproducible to $\pm$1 nm.

In the bimane assay of topography, the emission wavelength of bimane-labeled residues is measured. This parameter is sensitive to exposure of bimane to aqueous solution. The $\lambda_{max}$ of the bimane emission is red-shifted when exposed to an aqueous environment and blue-shifted when buried in the lipid bilayer (*1*, *3*). In the BODIPY assay, the exposure of BODIPY-labeled residues to externally added anti-BODIPY antibodies is measured (*1*, *3*). Binding of anti-BODIPY antibody to BODIPY results in quenching of BODIPY fluorescence. The intensity of fluorescence from BODIPY groups that are highly exposed to aqueous solution can be quenched 50−60% upon antibody binding (*1*, *3*). BODIPY groups that are buried within the bilayer show decreased quenching. In addition, anti-BODIPY antibodies cannot quench BODIPY groups exposed to the aqueous solution on the internal (trans) surface of the bilayer, because the antibody is too large to pass though either the lipid bilayer or pores formed by the T domain (*2*, *3*, *21*).

*Behavior of TH1−TH3 Region in Solution at Neutral and Low pH.* First, the fluorescence emission of bimane-labeled Cys mutants was monitored for the T domain in the native, neutral pH conformation (Figure 1A). All of the labeled residues in the TH1−TH3 region showed moderately (465−

470 nm) or strongly (470−480 nm) red-shifted fluorescence at neutral pH. This shows that the labeled groups were exposed to solution. Consistent with this conclusion, these residues were also strongly quenched by anti-BODIPY antibodies (>60% quenching) with the exception of residue 213 [about 40% quenching (Figure 1B)]. This latter result is consistent with the fact that residue 213 is less exposed to solution than the other residues studied as judged from the crystal structure of the native T domain (*4*).

When incubated in solution at low pH, which causes the T domain to undergo a conformational change that allows it to penetrate lipid bilayers (*41*), a number of residues exhibited a significant change in exposure to solution. Residues 210 and 211 became less exposed to solution as shown both by a blue shift (average of 3 nm) in the bimane emission and a loss in anti-BODIPY antibody quenching (from about 80 to 40%) (parts A and B of Figure 1). In contrast, residues 213, 216, and 218 showed an increase in exposure to aqueous solution, as shown by a red shift in the bimane emission (average of 5 nm). In addition, a 15−25% increase in anti-BODIPY antibody quenching was observed for residues 213 and 216 (parts A and B of Figure 1). These changes are consistent with a partial inside-out twisting of TH1 (see the Discussion).

The remaining residues in TH1, TH2, and TH3 showed small, relatively ambiguous changes in exposure to solution at low pH as judged by bimane fluorescence and anti-BODIPY antibody quenching (Figure 1).

*Topography of TH1−TH3 in the Bilayer-Inserted T Domain.* Bimane fluorescence measurements were also made on the model membrane-inserted T domain. Figure 2A shows a comparison of bimane emission $\lambda_{max}$ for T domain in solution at low pH (open bars) and when inserted into SUVs composed of 30 mol % DOPG/70 mol % DOPC at low pH (shaded bars). Most residues studied showed a moderate−strong blue shift upon insertion into SUVs. This shows that residues along the entire TH1−TH3 sequence interact with the lipid bilayer at low pH. Residues 213, 216, 218, and 254 exhibited very strongly blue-shifted fluorescence, consistent with membrane insertion involving some degree of penetration into the hydrophobic core of the lipid bilayer. Only residue 211 showed a red shift upon T domain membrane insertion.

The interaction between TH1−TH3 and the lipid bilayer was confirmed by changes in anti-BODIPY antibody binding. With the exception of residue 211, all residues showed a reduced degree of reaction with anti-BODIPY antibody upon T domain membrane insertion. In agreement with the bimane results, residues 213, 216, and 218 showed a particularly low degree of antibody binding when lipid was bound. Residue 254 also showed a significantly reduced degree of antibody binding in the presence of lipid but no more than several other residues.

We next compared the behavior of T domain inserted into DOPG/DOPC vesicles to those for T domain inserted into DOPG/DMoPC vesicles. Previous studies showed that the hydrophobic helices of the T domain (TH5−TH9) insert much more deeply into DOPG/DMoPC vesicles (in which the TM conformation forms) than they do into DOPG/DOPC vesicles (in which the shallowly inserted P conformation forms) (*1*, *3*, *22*). However, we found that the TH1−TH3 insertion depth is the same in these two lipid mixtures. As shown in parts A and B of Figure 3, there was no marked significant difference between the conformation of these sequences as judged either by bimane emission and anti-BODIPY antibody binding.

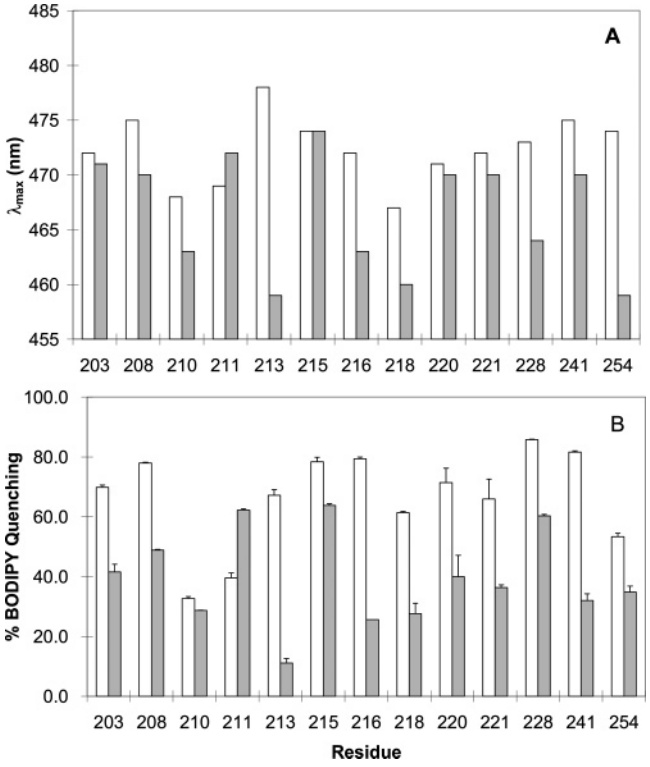


FIGURE 2: Fluorescence properties of labeled T domain in solution at low pH and when membrane-inserted. (A) Emission $\lambda_{max}$ of bimane fluorescence for labeled T domain in solution at pH 4.3 (open bars) or bound at pH 4.3 to SUVs composed of 7:3 DOPC/DOPG (mol/mol) (shaded bars). (B) Anti-BODIPY quenching of BODIPY fluorescence with labeled T domain in solution at pH 4.3 (open bars) or bound at pH 4.3 to SUVs composed of 7:3 DOPC/DOPG (mol/mol) (shaded bars). Numbers on the *x* axis indicate positions of labeled Cys residues. Data for the T domain in solution are from Figure 1.

These experiments were repeated for the same set of residues under two other conditions that give rise to the formation of the TM conformation by T domain inserted into DOPG/DOPC vesicles at low pH: a higher T domain concentration and the presence of a molten-globule state protein (HSA) (*1*, *3*). In both cases, the results were very similar to those obtained for the T domain inserted into vesicles composed of DOPG/DMoPC (data not shown).

*Direct Measurement of Insertion Depth by Fluorescence Quenching.* Previous studies have shown that blue-shifted fluorescence and low anti-BODIPY antibody binding observed upon membrane insertion are a result of the burial of the labeled residues within the lipid bilayer (*1*−*3*). To confirm this, a dual fluorescence quenching method that measures the depth of fluorescent groups in membranes was used (*17*). The basis of this method is that fluorescent groups exposed to solution are strongly quenched by an aqueous quencher (iodide), giving a high value of $F_o/F_{KI} - 1$, while deeply inserted groups are strongly quenched by a membrane-inserted hydrophobic quenching molecule (10-DN), giving a high value of $F_o/F_{10-DN} - 1$ (see the Experimental Procedures). Because the accessibility to any single quencher could be affected by local protein conformation, the most accurate measure of depth is given by the ratio of the

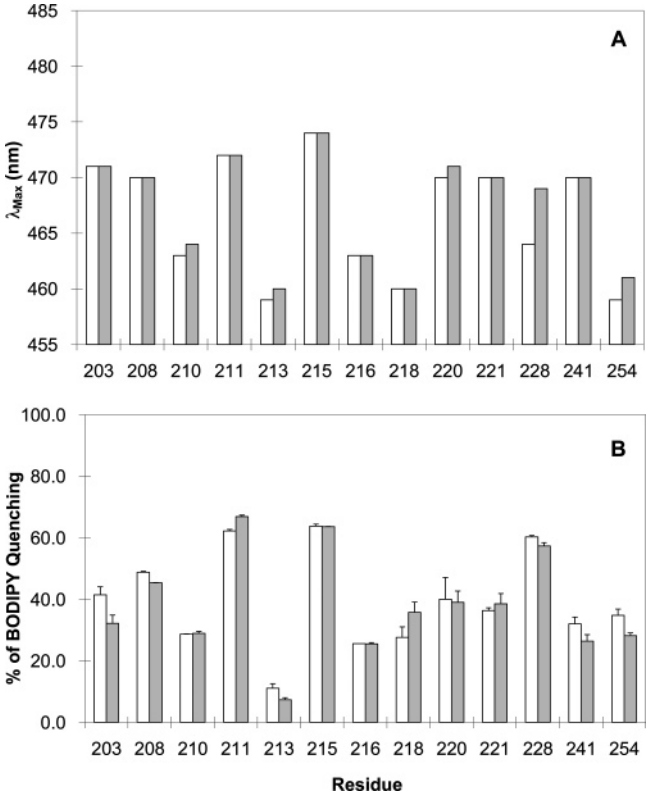


FIGURE 3: Fluorescence properties of membrane-inserted T domain at low pH. (A) Emission $\lambda_{max}$ of bimane fluorescence for labeled T domain bound to SUVs composed of 7:3 (mol/mol) DOPC/DOPG (open bars) or DMoPC/DOPG (shaded bars) at pH 4.3. (B) Anti-BODIPY quenching of BODIPY fluorescence of labeled T domain bound to SUVs composed of 7:3 (mol/mol) DOPC/DOPG (open bars) or DMoPC/DOPG (shaded bars) at pH 4.3. Numbers on the *x* axis indicate positions of labeled Cys residues. Data for the T domain bound to DOPC/DOPG are from Figure 2.

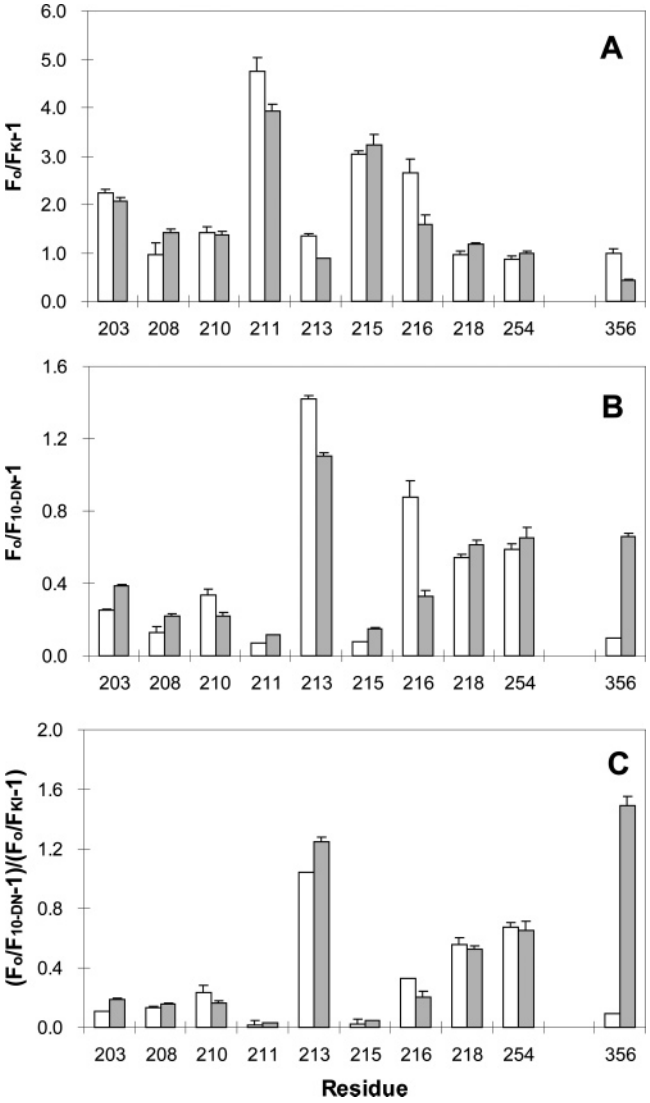


FIGURE 4: Dual quenching assay results for bimane-labeled T domain residues in T domain inserted into vesicles at pH 4.3. (A) Iodide quenching of bimane fluorescence of vesicle-inserted labeled T domain. Samples contained T domain incorporated into SUVs composed of 7:3 DOPC/DOPG (mol/mol) (open bars) or DMoPC/DOPG (shaded bars) at pH 4.3. $F_o/F_{I^-}$ is the ratio of fluorescence in the absence of iodide ($F_o$) to that in the presence of 100 mM iodide ($F_{I^-}$) after the correction for dilution with iodide. (B) 10-DN quenching of bimane fluorescence of vesicle-inserted labeled T domain. Samples contained T domain incorporated into SUVs composed of 7:3 DOPC/DOPG (mol/mol) (open bars) or DMoPC/DOPG (shaded bars) with or without 7.8 mol % (for DMoPC/DOPG) or 10 mol % (for DOPC/DOPG) 10-DN at pH 4.3. $F_o/F_{10-DN}$ is the ratio of fluorescence in the absence of 10-DN ($F_o$) to that in the presence of 10-DN ($F_{10-DN}$). (C) Ratio of quenching by 10-DN to that by iodide. The higher the value, the deeper the residue is inserted within the bilayer. The behavior of residue 356 is shown as a control. It shallowly locates in DOPC-containing vesicles but deeply inserts in DMoPC-containing vesicles (*2*, *3*, *17*). The results shown are from samples prepared in triplicate.

quenching by these two probes, which is given by $(F_o/F_{10-DN} - 1)/(F_o/F_{KI} - 1)$. Quenching ratio data for TH1−TH3 residues in membrane-inserted T domain (Figure 4C) are in good agreement with the data obtained by bimane emission and anti-BODIPY antibody binding measurements. Residue 213 appeared to be the most deeply buried, and residues 216, 218, and 254 showed a moderate degree of burial within the bilayer. This was true in both DOPG/DOPC and DOPG/DMoPC vesicles. For reference, the behavior of residue 356, located in the middle of TH9, is shown (Figure 4C). In agreement with previous studies, this residue switches from a very shallow depth in DOPG/DOPC vesicles (P state) to a deeply inserted location in DOPG/DMoPC vesicles (TM state).

It should be noted that although both iodide and the lipid surface are anionic, any repulsion between them should not affect the above conclusions. As we pointed out previously (*17*), although repulsion may affect the level of quenching by iodide, similar conclusions concerning the depth of residues can be obtained by just considering quenching by iodide or by 10-DN (which is uncharged) individually (i.e., residues strongly quenched by 10-DN tend to be weakly quenched by iodide and vice versa).

*Distinguishing Exposure on the Cis and Trans Sides of the Bilayer through the Interaction between Biotinylated T Domain Residues and BOD−SA.* One remaining question is whether TH1−TH3 residues locate closer to the cis or trans surface of the bilayer. (The cis side is the side of the bilayer from which insertion occurs, in this case, the outer surface, and the trans side is the side to which the A chain is translocated, in this case, the inner surface.) To examine this question, we used our recently introduced assay based on the binding of biotinylated residues to BOD−SA located in the external solution (which occurs when residues are on the cis side of the bilayer) or trapped within the lumen of the vesicles (which occurs when residues are on the trans

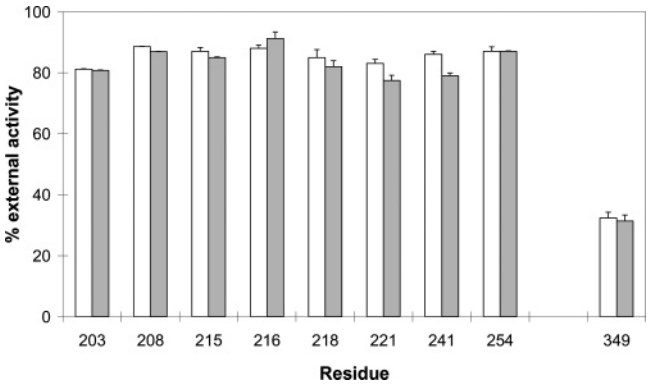


FIGURE 5: Percent external reactivity for biotinylated T domain mutants. Percent external reactivity is shown for a series of biotinylated T domain Cys mutants bound to LUVs without (open bars) or with (shaded bars) 0.2 $\mu$g/mL entrapped unlabeled SA. Samples contained 2 $\mu$g/mL total T domain (0.2 $\mu$g/mL biotinylated T domain and 1.8 $\mu$g/mL unlabeled WT T), 0.2 $\mu$g/mL BOD−SA, and 0.19−0.22 mM lipid [7:3 (mol/mol) DOPC/DOPG LUV] at pH 4.3. The *x* axis numbers indicate the positions of the biotinylated Cys in the T domain sequence. Percent external reactivity = [amount of a residue exposed to the external vesicle surface/total amount exposed to the external and internal surfaces] × 100% (see the Experimental Procedures for details).

side of the bilayer) (*22*). Binding is detected by the increase in BODIPY fluorescence when biotin binds to BOD−SA and displaces the BODIPY group from the biotin-binding pocket (*42*−*44*).

Figure 5 shows the percent external reactivity as a function of the biotinylation site for the T domain inserted into DOPG/DOPC LUVs. [Note that the T domain tends to go into the TM state when inserting into LUVs (*23*).] Percent external reactivity = [the amount of reaction with external BOD−SA/total reaction with external and trapped BOD−SA] × 100%. A residue that is only exposed on the external (cis) surface gives a percent external reactivity of 100%, while one that is exposed on the internal surface gives a percent external reactivity of 0%.

Figure 5 shows that all of the residues tested within the TH1−TH3 region gave a percent external reactivity of 80−90%. This indicates that the TH1−TH3 region is predominantly located on the external surface. [Previous data has shown that small percent reactivity with trapped SA is due to a minor population with an inverted orientation (*22*).] As a control, percent external reactivity was measured for residue 349, which is in the loop connecting TH8 and TH9. This loop reaches the trans side of the bilayer to a significant degree (*22*). As expected, residue 349 exhibited a much lower percent external reactivity than the other residues studied. In contrast residue 293, which is in the exposed loop between TH5 and TH6, gave a percent external reactivity similar to that for TH1−TH3 residues, again in agreement with previous results (data not shown) (*22*).

Preincubation of T domain-containing samples with a population of vesicles containing trapped unlabeled SA did not affect binding to external BOD−SA (Figure 5). As demonstrated previously, this indicates that the TH1−TH3 region is not equilibrating back and forth across the bilayer. If it had been equilibrating across the bilayer, binding to trapped SA would have prevented binding to the externally added BOD−SA (*22*). Thus, the TH1−TH3 region locates close to the cis surface of the bilayer in a stable fashion.

## DISCUSSION

*Conformational Changes within TH1−TH3 in Aqueous Solution at Low pH.* Defining the structure of membrane-penetrating domains from α-helical-rich toxins is a challenging problem because their behavior is more complex than that of standard integral membrane proteins. Under conditions that promote membrane insertion, these domains tend to form partly unfolded states in solution, and when membrane-inserted can exist in more than one conformation (*2*, *10*, *28*). In addition, their hydrophobic helices can form atypical topographies not observed in normal membrane proteins (*1*). This complexity may be related to the functional roles of these domains, which require large conformational changes during the membrane insertion and protein translocation processes.

Our strategy to investigate T domain structure has been to define the conditions under which different conformations predominate and then use several fluorescence techniques to define topography. In previous studies, we concentrated upon the hydrophobic helices of the T domain. In this study, we completed defining T domain topography by examining its hydrophilic N-terminal helices.

Upon exposure to low pH, moderate changes in the exposure of residues in the TH1−TH3 region were observed for the T domain in solution. This is consistent with the model of Zhan et al., who proposed that upon incubation at low pH the three helical layers of the T domain (TH1−TH4, TH5−TH7, and TH8−TH9) come apart to a small degree (*41*). [It should be noted that previous studies show T domain secondary structure in solution remains highly helical both at neutral and low pH (*1*, *45*).]

A more detailed exposure profile was obtained for TH1 because several studies suggest that it has an important role in the translocation process (*37*−*39*). A significant conformational change was observed within TH1 at low pH. This appears to involve an inside-out twisting of TH1 relative to the rest of the T domain such that the exposure of residues in the central portion of the helix changes. Some residues facing the interior of the T domain at neutral pH become exposed to solution at low pH, while other residues exposed to solution at neutral pH become more buried within the interior of the protein. This change should aid T domain insertion into membranes, because it exposes the hydrophobic surface of TH1. Low pH also increases the exposure of T domain hydrophobic helices to solution (*41*). Therefore, an overall effect of low pH is to facilitate T domain insertion into membranes by altering the T domain conformation in a fashion that exposes hydrophobic residues all along the T domain sequence.

*Conformation of TH1−TH3 upon T Domain Insertion into Lipid Bilayers.* Membrane insertion of the T domain is known to result in a number of changes in the T domain structure. These include an apparent increase in overall α helix content and interaction of hydrophobic helices TH5−TH9 with the lipid bilayer (*1*−*3*, *16*, *22*, *28*, *34*, *46*). When we examined the properties of TH1−TH3 in the T domain that was inserted into lipid vesicles at low pH, a blue shift was observed for 11 of 13 bimane-labeled residues, while 12 of 13 BODIPY-labeled residues exhibited a significant decrease in binding to anti-BODIPY antibodies. This shows that there is an extensive interaction of residues all along

the TH1−TH3 region with the lipid bilayer. Quenching by iodide and 10-DN confirms that this involves some degree of penetration of the lipid bilayer. However, a comparison to our previous studies shows that the overall insertion of TH1−TH3 is significantly shallower than that of the more hydrophobic C-terminal TH5−TH9 helices for the T domain in the deeply inserted TM state (*1*, *3*).

A more detailed picture was obtained for TH1, which is the most hydrophobic of the N-terminal helices. As judged by bimane emission and antibody binding, four (210, 213, 216, and 218) of nine residues in TH1 inserted somewhat deeply within the bilayer, with residue 213 inserting very deeply. Two residues (211 and 215) insert very shallowly. These conclusions were confirmed by the experiments with aqueous and membrane-inserted quenchers. These data are consistent with a structure in which the hydrophobic side of the N-terminal two thirds of TH1 is in contact with the core of the lipid bilayer. Interestingly, the amphiphilic N-terminal helix (residues 347−364) of the pore-forming domain of colicin E1 (p190), which is analogous to TH1 in some respects, has very recently been shown to form a classical amphiphilic helix along the membrane surface (*47*). The colicin E1 pore-forming domain N-terminal helix has a more extensive hydrophobic face than TH1 (*47*).

Biotinylated T domain residues all along the TH1−TH3 sequence were exposed to externally added BOD−SA to a much greater degree than they were to BOD−SA trapped in the vesicle lumen. This means that the TH1−TH3 region lies primarily on the cis surface of bilayer. In combination with previous studies that show that most of the hydrophilic loops in the TH5−TH9 region also lie on the cis side of the bilayer, this suggests that the topography of the membrane-inserted T domain at low pH represents a pretranslocation structure, in which the A chain attached to TH1 would be on the cis side of the bilayer (see below).

*TH1−TH3 Insertion Is Not Sensitive to Conformational Changes in TH5−TH9.* As noted above, we previously demonstrated that the hydrophobic TH5−TH9 portion of the T domain can adopt two distinct conformations (*1*, *2*, *3*, *27*, *28*). In the shallowly inserted conformation (P state), the entire TH5−TH9 region lies close to the cis surface of the bilayer, while in the more deeply inserted conformation (TM state), TH8 and TH9 form a transmembraneous hairpin connected by a tight turn (*3*). In the TM state, helices TH5−TH7 also insert much more deeply but not in the TM form (*1*). (The TM state refers to a state in which *some* of the helices of the T domain form a TM structure.) TH5−TH7 and TH8−TH9 interact in this more deeply inserting state, as shown by the fact that mutations in the TH8−TH9 hairpin disrupt deep insertion of residues in the TH5−TH7 region (*34*).

The present study shows that the N terminal TH1−TH3 region does not undergo a conformational change under conditions in which the TH5−TH9 region changes from the P to TM state. As a consequence, TH1−TH3 does not insert as deeply as the TH5−TH9 region in the TM state (Figure 6). The lack of an effect of the TH5−TH9 conformation upon the TH1−TH3 conformation suggests that in the membrane-inserted state TH1−TH3 is unlikely to interact strongly with the remainder of the T domain. [Interestingly, we previously found that TH4, which is also part of the hydrophilic helix layer, does insert more deeply in the TM state (*1*), suggesting that it is affected by the interaction with TH5−TH9.]

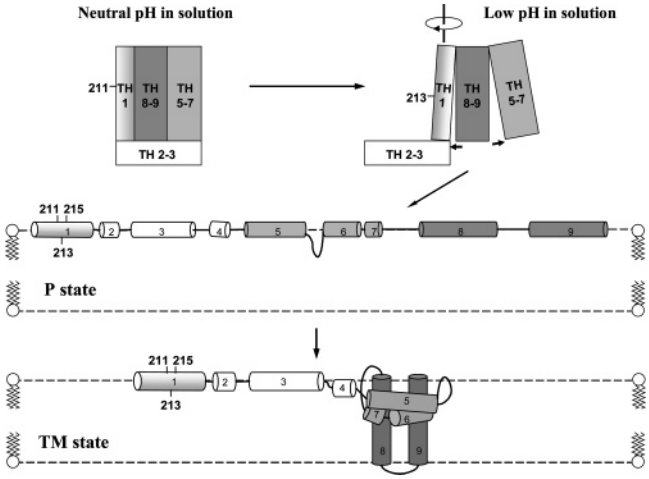


FIGURE 6: Schematic illustration of T domain conformations. TH1−TH9 represent helices 1−9 in the crystal structure (*4*). (Top left) T domain in solution at neutral pH. The helical layers in the native structure are shown in their appropriate orientations. TH4 is at the back of the structure and cannot be seen. (Top right) T domain in solution at low pH based on the data for TH1−TH3 obtained in this paper and from previous studies of TH4−TH9 (*41*). The three helical layers come apart at low pH, and TH1 twists to expose its hydrophobic surface. (Middle) Membrane-inserted T domain in surface conformation (P state) at low pH, showing the locations of TH1−TH3 defined in this paper. (Bottom) Membrane-inserted T domain in transmembraneous conformation (TM state) at low pH, showing the locations of TH1−TH3 defined in this paper. The positions shown for TH4−TH9 within the bilayer derive from previous studies (see the text for details) (*1*, *3*, *34*). Darker shading of sequences represents greater hydrophobicity.

*Model for T Domain Conformational Changes at Low pH in Solution and upon Membrane Insertion.* The hydrophilic helices of the T domain are likely to have an important role in inducing the conformational changes observed at low pH. TH1−TH4 contain most of the charged residues found in the T domain. They have slightly more acidic than basic residues and are likely to carry a slight net negative charge at neutral pH. However, at low pH, this region should have a strong net positive charge (*8*), and repulsion between cationic residues, both within TH1−TH4 and between TH1−TH4 and TH5−TH9 residues, could induce the partial unfolding of the T domain observed at low pH (*41*). Low pH-induced breakdown of favorable Coulombic interactions between spacially close residue pairs that have opposite charge at neutral pH (Arg210−Glu362, Lys216−Glu259, Lys229−Glu249, and Glu292−Lys299) may also contribute to unfolding. Finally, changes in hydrogen bonding between side chains and backbone groups, analogous to changes that have been observed for residues in colicin E1, may also play an important role in this process (*48*).

Figure 6 (top) schematically summarizes the low pH-induced changes in the conformation of the TH1−TH3 region in solution. The most significant change involves an alteration of the way TH1 is positioned relative to the remainder of the T domain. As noted above, there is a twist such that the buried hydrophobic face of the N-terminal two thirds of TH1 becomes more exposed to a polar environment, while the more hydrophilic face becomes more buried in a hydrophobic environment. It is less clear what change, if any, is occurring in the remainder of TH1 or TH2−TH3. We did not detect a change in the exposure of residues on

helices TH2 and TH3 at low pH in solution, but useful information was only obtained for two residues; thus, it is possible that there are changes that we missed. The previously observed increased exposure of hydrophobic helices at low pH (*41*) suggests that the interactions between TH2−TH3 and hydrophobic helices TH5−TH9 are weakened or lost. It is possible that this can be explained by the twist in the TH1 conformation, resulting in a turning of TH2−TH3 such that their contact with TH5−TH9 is lost at low pH (top of Figure 6).

Upon membrane insertion, the conformational changes that occur in TH1 upon exposure to low pH in solution are largely reversed, such that residue 213, which becomes exposed to a polar environment at low pH, now becomes buried in the bilayer, while residue 211, which moves into a more hydrophobic environment at low pH, now becomes more exposed to aqueous solution. In other words, the location of these residues relative to the hydrophobic core of the lipid bilayer in the membrane-inserted T domain is reminiscent of their location relative to the hydrophobic core of the T domain in its native, neutral pH solution conformation. We interpret the changes in the T domain conformation at low pH in solution as preparing TH1 for insertion by inducing exposure of buried residues so that they can interact with the lipid bilayer in a subsequent step.

Upon T domain insertion, residues in helices TH2 and TH3 also move into a more hydrophobic environment, indicating that these residues interact with the lipid bilayer. In combination with our previous data showing that residues in helix TH4 also interact with the lipid bilayer (*1*), this indicates that all of the more hydrophilic helices of the T domain interact with the lipid bilayer at low pH.

Combining the information on the behavior of TH1−TH3 with that in our previous studies of the more hydrophobic helices of the T domain allows us to propose a model for the conformation of the entire membrane-inserted T domain (middle and bottom of Figure 6). In the P state, the entire T domain sequence lies along the membrane surface.[1] In the TM state, TH1−TH3 remain near the bilayer surface but TH4−TH9 become more deeply buried, with TH8−TH9 forming a TM hairpin. As noted above, the change in the TH4−TH9 conformation upon changing from the P to TM state is not accompanied by a change in the TH1−TH3 conformation, suggesting that the hydrophilic TH1−TH3 and hydrophobic TH5−TH9 subdomains do not interact strongly after membrane insertion. This may have important implications for translocation (see below).

*Comparison of the Model for T Domain Topography to Models Derived from Other Methods.* Some previous models for T domain topography have been based on proteolysis and cross-linking to hydrophobic photolabels (*16*, *46*, *49*). These approaches defined some of the sequences interacting with the lipid bilayer and agree with our fluorescence results in terms of helix burial in the lipid bilayer, decreasing in the order TH8−TH9 > TH5−TH7 > TH2−TH4. Both these nonfluorescence based methods and our fluorescence-based approach [including our previous experiments using native fluorescence of Trp 206 (*28*)] show that some residues in TH1 insert deeply.

The fluorescence measurements in this study add significant, new information concerning TH1−TH3, including the orientation of membrane-bound TH1 and the observation that interactions with the lipid bilayer occur all along the TH1−TH3 sequence. In addition, proteolysis and photolabeling did not distinguish between a TM and non-TM topography for TH1, while fluorescence reveals a non-TM topography. However, our fluorescence study involves the isolated T domain, while previous studies involved the whole toxin. Preliminary studies using the T domain linked to the A chain suggest that membrane penetration by TH1 may be greater than in the isolated T domain (data not shown).

The agreement between different methods suggests that the fluorescence labels used in this study are unlikely to be highly perturbing. The observation that several different types of fluorescence labels report the same conformational differences between the T domain in solution at neutral pH and the T domain in solution at low pH supports this conclusion (*1*, *28*, *41*). The observation that different fluorescent labels and native Trp fluorescence, in which probe perturbation is not an issue, all distinguish between the P and TM states also suggests that labeling is not highly perturbing (*3*, *28*). In addition, a lack of significant perturbation of the protein structure by bimane groups has been directly demonstrated in previous studies (*50*). Nevertheless, there can be serious perturbation when a label is introduced within a folded protein at a buried site where it cannot be easily accommodated. We believe this is happening in the native T domain in the case of residues 220 and 254. Both of these residues should be buried according to the crystal structure of the T domain, and consistent with this, both were difficult to label (not shown); however, labels attached to these residues appeared to be relatively solution-exposed in the native protein at neutral pH. In addition, we do not rule out the possibility that labeling may affect the precise depth of membrane-inserted helices.

It should be pointed out that Senzel et al. have proposed a model for the T domain structure that is very different from that defined in this paper. They detect an open-pore conformation, which corresponds to a post-translocation state, in which N-terminal helices 1−4 have reached the trans side of the bilayer. Because their conformation is detected on the basis of its activity, it might represent only a small fraction of the total membrane-inserted T domain. In contrast, our experiments would tend to detect the predominant conformation. Alternately, the conformation that we detect and that was detected by Senzel et al. might predominate under different experimental conditions (there was a transmembrane pH gradient in the experiments of Senzel et al.). In any case, our structure clearly represents a pretranslocation conformation, in which the N-terminal part of the T domain (to which the A chain would normally be attached) has not yet crossed the bilayer, while that of Senzel et al. is a post-translocation state.

*Potential Role of TH1−TH3 in A Chain Translocation.* As noted above, TH1 aids T domain insertion. Previous studies show that TH1 also has an important role in

[1] It is interesting that the comparison to previous studies suggests that residues within the hydrophobic helices are much more uniformly exposed to aqueous solution in the P state than residues in the hydrophilic helices (*1*−*3*). We interpret this to mean that the labeling groups, which are somewhat polar (*1*−*3*), can twist uniformly hydrophobic helices to allow the labels to face aqueous solution but cannot easily twist helices with many hydrophilic groups because that would result in the burial of polar and charged residues.

translocation. Truncation of amino-terminal residues in TH1 beyond residue 205 affected the ability of the B chain to form ion channels at low pH (*51*). Amino acid substitution experiments have suggested that the overall amphiphilic nature of the TH1 helix may be functionally important, although its exact sequence may not be critical (*38*). The more highly hydrophilic surface on TH1 may interact with the A chain and/or the rest of the T domain (*39*), although the sign of the charge on TH1 residues seems to have a minimal effect on its function (*38*). In combination with our observations showing that TH1−TH3 do not interact tightly with the hydrophobic sequences that form the remainder of the T domain, these observations suggest some plausible models for the role of TH1−TH3 in translocation. For example, TH1−TH3 may form a flexible tether. This could be important for translocation. It is known that the C-terminal part of the A chain is the first portion of the A chain to cross the bilayer during translocation (*36*), and this requires that some portion of the T domain also crosses the bilayer early in the translocation process. In fact, the model of Senzel et al. for the conformation of the T domain after translocation proposes that both the A chain and the entire TH1−TH4 sequence translocates (*52*). Our results are consistent with a model in which some or all of TH1−TH3 translocates simultaneously with the A chain. Alternately, TH1−TH3 may form part of the translocation pathway for the A chain, such that most of TH1−TH3 translocation occurs after A chain translocation. In either case, TH1−TH3 might aid translocation by interacting with the translocating A chain and helping to align/orient it in a fashion that lowers the energy barrier for translocation. It should be noted that these models do not rule out a role of cytosolic factors in aiding the later steps in the translocation process (*25*).

Further studies on how the A chain affects the topography of the T chain should provide additional insights into the role of TH1−TH3 in translocation. The impact of mutations in TH1−TH3 residues upon T domain topography and A chain translocation should also be informative.

## REFERENCES


1. Rosconi, M. P., and London, E. (2002) Topography of helices 5−7 in membrane-inserted diphtheria toxin T domain: Identification and insertion boundaries of two hydrophobic sequences that do not form a stable transmembrane hairpin, *J. Biol. Chem. 277*, 16517−16527.
2. Wang, Y., Malenbaum, S. E., Kachel, K., Zhan, H., Collier, R. J., and London, E. (1997) Identification of shallow and deep membrane-penetrating forms of diphtheria toxin T domain that are regulated by protein concentration and bilayer width, *J. Biol. Chem. 272*, 25091−25098.
3. Kachel, K., Ren, J., Collier, R. J., and London, E. (1998) Identifying transmembrane states and defining the membrane insertion boundaries of hydrophobic helices in membrane-inserted diphtheria toxin T domain, *J. Biol. Chem. 273*, 22950−22956.
4. Choe, S., Bennett, M. J., Fujii, G., Curmi, P. M., Kantardjieff, K. A., Collier, R. J., and Eisenberg, D. (1992) The crystal structure of diphtheria toxin, *Nature 357*, 216−222.
5. Tsuneoka, M., Nakayama, K., Hatsuzawa, K., Komada, M., Kitamura, N., and Mekada, E. (1993) Evidence for involvement of furin in cleavage and activation of diphtheria toxin, *J. Biol. Chem. 268*, 26461−26465.
6. Chiron, M. F., Fryling, C. M., and FitzGerald, D. J. (1994) Cleavage of pseudomonas exotoxin and diphtheria toxin by a furin-like enzyme prepared from beef liver, *J. Biol. Chem. 269*, 18167−18176.
7. Naglich, J. G., Metherall, J. E., Russell, D. W., and Eidels, L. (1992) Expression cloning of a diphtheria toxin receptor: Identity with a heparin-binding EGF-like growth factor precursor, *Cell 69*, 1051−1061.
8. London, E. (1992) Diphtheria toxin: Membrane interaction and membrane translocation, *Biochim. Biophys. Acta 1113*, 25−51.
9. Pappenheimer, A. M., Jr. (1977) Diphtheria toxin, *Annu. Rev. Biochem. 46*, 69−94.
10. Blewitt, M. G., Chung, L. A., and London, E. (1985) Effect of pH on the conformation of diphtheria toxin and its implications for membrane penetration, *Biochemistry 24*, 5458−5464.
11. Hu, V. W., and Holmes, R. K. (1984) Evidence for direct insertion of fragments A and B of diphtheria toxin into model membranes, *J. Biol. Chem. 259*, 12226−12233.
12. Zhao, J. M., and London, E. (1988) Conformation and model membrane interactions of diphtheria toxin fragment A, *J. Biol. Chem. 263*, 15369−15377.
13. Silverman, J. A., Mindell, J. A., Finkelstein, A., Shen, W. H., and Collier, R. J. (1994) Mutational analysis of the helical hairpin region of diphtheria toxin transmembrane domain, *J. Biol. Chem. 269*, 22524−22532.
14. Tortorella, D., Sesardic, D., Dawes, C. S., and London, E. (1995) Immunochemical analysis shows all three domains of diphtheria toxin penetrate across model membranes, *J. Biol. Chem. 270*, 27446−27452.
15. Quertenmont, P., Wolff, C., Wattiez, R., Vander Borght, P., Falmagne, P., Ruysschaert, J. M., and Cabiaux, V. (1999) Structure and topology of diphtheria toxin R domain in lipid membranes, *Biochemistry 38*, 660−666.
16. D'Silva, P. R., and Lala, A. K. (2000) Organization of diphtheria toxin in membranes. A hydrophobic photolabeling study, *J. Biol. Chem. 275*, 11771−11777.
17. Hayashibara, M., and London, E. (2005) Topography of diphtheria toxin A chain inserted into lipid vesicles, *Biochemistry 44*, 2183−2196.
18. Oh, K. J., Senzel, L., Collier, R. J., and Finkelstein, A. (1999) Translocation of the catalytic domain of diphtheria toxin across planar phospholipid bilayers by its own T domain, *Proc. Natl. Acad. Sci. U.S.A. 96*, 8467−8470.
19. Kagan, B. L., Finkelstein, A., and Colombini, M. (1981) Diphtheria toxin fragment forms large pores in phospholipid bilayer membranes, *Proc. Natl. Acad. Sci. U.S.A. 78*, 4950−4954.
20. Sharpe, J. C., Kachel, K., and London, E. (1999) The effects of inhibitors upon pore formation by diphtheria toxin and diphtheria toxin T domain, *J. Membr. Biol. 171*, 223−233.
21. Sharpe, J. C., and London, E. (1999) Diphtheria toxin forms pores of different sizes depending on its concentration in membranes: Probable relationship to oligomerization, *J. Membr. Biol. 171*, 209−221.
22. Rosconi, M. P., Zhao, G., and London, E. (2004) Analyzing topography of membrane-inserted diphtheria toxin T domain using BODIPY-streptavidin: At low pH, helices 8 and 9 form a transmembrane hairpin but helices 5−7 form stable nonclassical inserted segments on the cis side of the bilayer, *Biochemistry 43*, 9127−9139.
23. Ren, J., Kachel, K., Kim, H., Malenbaum, S. E., Collier, R. J., and London, E. (1999) Interaction of diphtheria toxin T domain with molten globule-like proteins and its implications for translocation, *Science 284*, 955−957.
24. Hammond, K., Caputo, G. A., and London, E. (2002) Interaction of the membrane-inserted diphtheria toxin T domain with peptides and its possible implications for chaperone-like T domain behavior, *Biochemistry 41*, 3243−3253.
25. Ratts, R., Trujillo, C., Bharti, A., vanderSpek, J., Harrison, R., and Murphy, J. R. (2005) A conserved motif in transmembrane helix 1 of diphtheria toxin mediates catalytic domain delivery to the cytosol, *Proc. Natl. Acad. Sci. U.S.A. 102*, 15635−15640.
26. Ratts, R., Zeng, H., Berg, E. A., Blue, C., McComb, M. E., Costello, C. E., vanderSpek, J. C., and Murphy, J. R. (2003) The cytosolic entry of diphtheria toxin catalytic domain requires a host cell cytosolic translocation factor complex, *J. Cell Biol. 160*, 1139−1150.
27. Ren, J., Sharpe, J. C., Collier, R. J., and London, E. (1999) Membrane translocation of charged residues at the tips of hydrophobic helices in the T domain of diphtheria toxin, *Biochemistry 38*, 976−984.
28. Malenbaum, S. E., Collier, R. J., and London, E. (1998) Membrane topography of the T domain of diphtheria toxin probed with single tryptophan mutants, *Biochemistry 37*, 17915−17922.
29. Huynh, P. D., Cui, C., Zhan, H., Oh, K. J., Collier, R. J., and Finkelstein, A. (1997) Probing the structure of the diphtheria toxin

channel. Reactivity in planar lipid bilayer membranes of cysteine-substituted mutant channels with methanethiosulfonate derivatives, *J. Gen. Physiol. 110*, 229−242.
30. Senzel, L., Gordon, M., Blaustein, R. O., Oh, K. J., Collier, R. J., and Finkelstein, A. (2000) Topography of diphtheria toxin's T domain in the open channel state, *J. Gen. Physiol. 115*, 421−434.
31. Kaul, P., Silverman, J., Shen, W. H., Blanke, S. R., Huynh, P. D., Finkelstein, A., and Collier, R. J. (1996) Roles of Glu 349 and Asp 352 in membrane insertion and translocation by diphtheria toxin, *Protein Sci. 5*, 687−692.
32. Mindell, J. A., Silverman, J. A., Collier, R. J., and Finkelstein, A. (1994) Structure−function relationships in diphtheria toxin channels: III. Residues which affect the cis pH dependence of channel conductance, *J. Membr. Biol. 137*, 45−57.
33. Silverman, J. A., Mindell, J. A., Zhan, H., Finkelstein, A., and Collier, R. J. (1994) Structure−function relationships in diphtheria toxin channels: I. Determining a minimal channel-forming domain, *J. Membr. Biol. 137*, 17−28.
34. Zhao, G., and London, E. (2005) Behavior of diphtheria toxin T domain containing substitutions that block normal membrane insertion at Pro345 and Leu307: Control of deep membrane insertion and coupling between deep insertion of hydrophobic subdomains, *Biochemistry 44*, 4488−4498.
35. Finkelstein, A., Oh, K. J., Senzel, L., Gordon, M., Blaustein, R. O., and Collier, R. J. (2000) The diphtheria toxin channel-forming T-domain translocates its own $NH_2$-terminal region and the catalytic domain across planar phospholipid bilayers, *Int. J. Med. Microbiol. 290*, 435−440.
36. Falnes, P. O., and Olsnes, S. (1995) Cell-mediated reduction and incomplete membrane translocation of diphtheria toxin mutants with internal disulfides in the A fragment, *J. Biol. Chem. 270*, 20787−20793.
37. vanderSpek, J. C., Mindell, J. A., Finkelstein, A., and Murphy, J. R. (1993) Structure/function analysis of the transmembrane domain of DAB389-interleukin-2, an interleukin-2 receptor-targeted fusion toxin. The amphipathic helical region of the transmembrane domain is essential for the efficient delivery of the catalytic domain to the cytosol of target cells, *J. Biol. Chem. 268*, 12077−12082.
38. vanderSpek, J. C., Howland, K., Friedman, T., and Murphy, J. R. (1994) Maintenance of the hydrophobic face of the diphtheria toxin amphipathic transmembrane helix 1 is essential for the efficient delivery of the catalytic domain to the cytosol of target cells, *Protein Eng. 7*, 985−989.
39. Madshus, I. H. (1994) The N-terminal α-helix of fragment B of diphtheria toxin promotes translocation of fragment A into the cytoplasm of eukaryotic cells, *J. Biol. Chem. 269*, 17723−17729.
40. Bradford, M. M. (1976) A rapid and sensitive method for the quantitation of microgram quantities of protein utilizing the principle of protein−dye binding, *Anal. Biochem. 72*, 248−254.
41. Zhan, H., Choe, S., Huynh, P. D., Finkelstein, A., Eisenberg, D., and Collier, R. J. (1994) Dynamic transitions of the transmembrane domain of diphtheria toxin: Disulfide trapping and fluorescence proximity studies, *Biochemistry 33*, 11254−11263.
42. Emans, N., Biwersi, J., and Verkman, A. S. (1995) Imaging of endosome fusion in BHK fibroblasts based on a novel fluorimetric avidin−biotin binding assay, *Biophys. J. 69*, 716−728.
43. Nicol, F., Nir, S., and Szoka, F. C., Jr. (1999) Orientation of the pore-forming peptide GALA in POPC vesicles determined by a BODIPY-avidin/biotin binding assay, *Biophys. J. 76*, 2121−2141.
44. Nir, S., Nicol, F., and Szoka, F. C., Jr. (1999) Surface aggregation and membrane penetration by peptides: Relation to pore formation and fusion, *Mol. Membr. Biol. 16*, 95−101.
45. Chenal, A., Savarin, P., Nizard, P., Guillain, F., Gillet, D., and Forge, V. (2002) Membrane protein insertion regulated by bringing electrostatic and hydrophobic interactions into play. A case study with the translocation domain of diphtheria toxin, *J. Biol. Chem. 277*, 43425−43432.
46. Cabiaux, V., Quertenmont, P., Conrath, K., Brasseur, R., Capiau, C., and Ruysschaert, J. M. (1994) Topology of diphtheria toxin B fragment inserted in lipid vesicles, *Mol. Microbiol. 11*, 43−50.
47. Musse, A. A., Wang, J., Deleon, G. P., Prentice, G. A., London, E., and Merrill, A. R. (2006) Scanning the membrane-bound conformation of helix 1 in the colicin E1 channel domain by site-directed fluorescence labeling, *J. Biol. Chem. 281*, 885−895.
48. Musse, A. A., and Merrill, A. R. (2003) The molecular basis for the pH-activation mechanism in the channel-forming bacterial colicin E1, *J. Biol. Chem. 278*, 24491−24499.
49. Quertenmont, P., Wattiez, R., Falmagne, P., Ruysschaert, J. M., and Cabiaux, V. (1996) Topology of diphtheria toxin in lipid vesicle membranes: A proteolysis study, *Mol. Microbiol. 21*, 1283−1296.
50. Mansoor, S. E., McHaourab, H. S., and Farrens, D. L. (2002) Mapping proximity within proteins using fluorescence spectroscopy. A study of T4 lysozyme showing that tryptophan residues quench bimane fluorescence, *Biochemistry 41*, 2475−2484.
51. Stenmark, H., Ariansen, S., Afanasiev, B. N., and Olsnes, S. (1992) Interactions of diphtheria toxin B-fragment with cells. Role of amino- and carboxyl-terminal regions, *J. Biol. Chem. 267*, 8957−8962.
52. Senzel, L., Huynh, P. D., Jakes, K. S., Collier, R. J., and Finkelstein, A. (1998) The diphtheria toxin channel-forming T domain translocates its own $NH_2$-terminal region across planar bilayers, *J. Gen. Physiol. 112*, 317−324.

BI060587F